To appear in Ap. J., January 2002

Quasar Spectral Slope Variability in the Optical Band

Dario Trèvese

Dipartimento di Fisica, Università di Roma "La Sapienza",
Piazzale A. Moro 2, I-00185 Roma, Italy, dario.trevese@roma1.infn.it, and
Dipartimento di Fisica, Università di Roma "Tor Vergata",
Via della Ricerca Scientifica 1, I-00133 Roma, Italy

and

Fausto Vagnetti

Dipartimento di Fisica, Università di Roma "Tor Vergata",
Via della Ricerca Scientifica 1, I-00133 Roma, Italy, fausto.vagnetti@roma2.infn.it

ABSTRACT

We performed a new analysis of B and R light curves of a sample of PG quasars. We confirm the variability-redshift correlation and its explanation in terms of spectral variability, coupled with the increase of rest-frame observing frequency for quasars at high redshift. The analysis of the instantaneous spectral slope for the whole quasar samples indicates both an inter-QSO and intra-QSO variability-luminosity correlation. Numerical simulations show that the latter correlation cannot be entirely due to the addition of the host galaxy emission to a nuclear spectrum of variable luminosity but constant shape, implying a spectral variability of the nuclear component. Changes of accretion rate are also insufficient to explain the amount of spectral variation, while hot spots possibly caused by local disk instabilities can explain the observations.

Subject headings: galaxies: active - galaxies: photometry - galaxies: Seyfert - quasars: general - quasars : variability

1. INTRODUCTION

Although variability plays a key role in constraining the size of the central engine of active galactic nuclei, yet its physical origin remains substantially unknown. Even restricting to the class of non-Blazar objects, the most diverse mechanism have been proposed in recent years, including gravitational lensing due to intervening matter (Hawkins 1996), supernovae explosions (Aretxaga, Cid Fernandes & Terlevich 1997), instabilities in the accretion disk (Kawaguchi et al. 1998) and star collisions (Torricelli-Ciamponi et al. 2000). For a small number of low redshift objects, a multi-wavelength monitoring with adequate time sampling and resolution allows the interpretation of changes of the spectral energy distribution (SED) in terms of an interplay of emission components with different spectral and variability properties (see Ulrich, Maraschi, and Urry (1997) for a general review and Courvoisier (1998) for the case of 3C273). In the near infrared-optical-UV bands, variability studies indicate a hardening of the spectrum in the bright phase (Cutri et al. 1985; Edelson, Krolik & Pike 1990; Kinney et al. 1991; Paltani & Courvoisier 1994). So far, however, most of the statistical information on AGN variability, derives from single-band light curves of magnitude limited samples of objects (Angione & Smith 1972; Bonoli et al. 1979; Hawkins 1983; Trèvese et al. 1989; Cristiani, Vio & Andreani 1990; Trèvese et al. 1994; Hook et al. 1994; Bershady, Trèvese & Kron 1998). In the case of magnitude limited samples the analysis is complicated by the strong luminosity-redshift (L-z) correlation, caused by the crowding of objects towards the limiting flux. As a consequence it is difficult to isolate any intrinsic variability-luminosity (v-L) and variability-redshift (v-z) correlation. Moreover, the results of these analyses depend on the specific variability index adopted, as shown by Giallongo, Trèvese & Vagnetti (1991) who found a positive v-z correlation through a variability index defined on the basis of the rest-frame structure function. The existence of an average increase of variability with redshift was later confirmed by Cristiani et al. (1996). It turns out to be consistent with the suggestion of Giallongo, Trèvese & Vagnetti (1991) that QSOs at high redshift appear more variable since they are observed at a higher rest-frame frequency, where the variability is stronger (hardening in the bright phase and vice versa). A direct statistical evidence of the spectral variability, in terms of an average change of the B-R color with the variation of the B magnitude, was found by Giveon et al. (1999) as part of a statistical analysis of the B and R light curves of a sample of PG QSOs. A similar evidence has been found by Trèvese, Kron, & Bunone (2001) for the faint QSO sample of SA 57 (Koo, Kron & Cudworth 1986). Unfortunately, most (if not all) of the variability mechanisms proposed so far imply a hardening of optical-UV spectrum in the bright phase, so that they cannot be discriminated on purely qualitative grounds. As a first step towards constraining variability models quantitatively Trèvese, Kron, & Bunone (2001) compared with the observations a simple model where both spectral slope changes and brightness variations are due to temperature changes of an emitting black body. In the present paper, we present a new analysis of the B and R light curves of a sample of PG QSOs made available by Giveon et al. (1999), we analyze the consistency with previous results, and consider possible different sources of spectral variability. The paper is organized as follows: in section

2 we summarize the characteristics of the Giveon et al. (1999) data, in section 3 we analyze the v-z correlation, in section 4 we discuss the parameters adopted for the spectral variation analysis, in section 5 we consider the effect of the host-galaxy on SED variations, in section 6 we compare the observed spectral variations with those produced by changes of the accretion rate, and discuss the consistency of the observations with a simple model consisting of hot spots on the accretion disk. Section 7 contains a summary and the conclusions. We adopt $H_o = 50$ km s^{-1} Mpc^{-1}, $\mathrm{q_o} = 0.5$, unless otherwise stated.

2. THE DATA

The present analysis is based on the light curves made available to the community by the Wise Observatory group (Giveon et al. 1999). The sample consist of 42 PG QSOs selected to be nearby, i.e. $z < 0.4$, and bright, i.e. $B < 16$ mag.

The observations were made in the Johnson-Cousins B and R bands with the 1 m Wise Observatory telescope. The total duration of the campaign was 7 years and the median observing interval of the objects was 39 days. The r.m.s. photometric uncertainty is ~ 0.01 mag and ~ 0.02 mag in the B and R bands respectively. We refer to the original paper of Giveon et al. (1999) for all details concerning observations, calibration etc. The full B and R light curves of the entire sample were made available in electronic form.

Giveon et al. (1999) present the analysis of the correlation of different variability properties with other properties like luminosity, redshift, radio power, various line intensities and the X-ray spectral slope. In particular they show a correlation between the color changes $\Delta(B-R)$ and the brightness variations ΔB and ΔR, corresponding to an average hardening of the spectrum in the bright phase (and vice versa). They do not find a correlation between variability and redshift, at variance with Giallongo, Trèvese & Vagnetti (1991), Trèvese et al. (1994), Cristiani et al. (1996), but they ascribe this to the difficulty of disentangling v-z, v-L and L-z correlations in the sample. We stress that this is made particularly difficult by the small redshift interval spanned by the sample. We perform a new analysis of both the v-z correlation and the spectral slope changes in the following sections. For these purposes we have dereddened the data, using the extinction calculator of the NASA Extragalactic Database (NED).

3. VARIABILITY-REDSHIFT CORRELATION

To measure the amplitude of variability we define, for each object, the first order structure function, as in Di Clemente et al. (1996) (but omitting the subscript "1"):

$$S(\tau, \Delta\tau) = [(\frac{\pi}{2}\overline{|m(t+\tau) - m(t)|}^2 - \sigma_n^2)]^{\frac{1}{2}} \tag{1}$$

where $m(t)$ is either the B or the R magnitude, t is the rest-frame time, τ is the time lag between the observations, σ_n is the relevant r.m.s. noise and the bar indicates the average taken over all the pairs of observations lying in the time interval $\tau \pm \Delta\tau$. In this definition we adopt the square average of the absolute values of the difference instead of the average of the square difference as in Di Clemente et al. (1996), since the former quantity is less sensitive to outliers (Hook et al. 1994). The $\pi/2$ factor normalizes S to the r.m.s. value in the case of a Gaussian distribution. The adopted value of $\Delta\tau$ is the result of a trade-off between time resolution and statistical uncertainty.

In the following we define four variability indices $S_i(\tau \pm \Delta\tau)$, with $i = B, R$, and $\tau = 0.3 \pm 0.09$ yr, 2.0 ± 0.6 yr. The subscripts B and R refer to the observing band and the values of τ and $\Delta\tau$ have been chosen for comparison with previous analyses (Di Clemente et al. 1996). None of these four indices shows a significant correlation with redshift when the whole sample is considered, confirming the result of Giveon et al. (1999).

However, to disentangle the v-L, v-z and L-z correlations, we can restrict the analysis to a magnitude bin $-23.5 < M_B < -22.5$, around the average absolute magnitude of the sample $< M_B >= -22.75$. The result is shown in Figure 1. In this case we find a v-z correlation coefficient $r_{v,z} = 0.39$, which is marginally significant ($P(> r) = 0.09$) despite the small number of objects (19) in the bin. To examine the dependence of variability on redshift we take the ensemble averages of the four variability indices defined above, over the same subsample of 19 objects. For each observing band we compute the average rest-frame observing frequency of the sample. To compare the result with Di Clemente et al. (1996) we must take into account the dependence of variability on magnitude. For this purpose, we reduce S by an amount $\Delta S = (\partial S/\partial M_B)\ \Delta M_B$ where for $S(M_B)$ we adopt model A of Cristiani et al. (1996) and ΔM_B is the difference between the average absolute magnitudes of the present sample and the sample of Di Clemente et al. (1996). Figure 2 shows the increase of variability with the observing frequency. At each frequency variability is larger for larger time lag τ (due to the increase of the structure function from $\tau = 0.3$ yr to $\tau = 2$ yr). The new points, obtained from the present analysis, are consistent with the previous results, which were obtained from different samples and observing frequencies. The general trend can be quantified as:

$$\partial S_i/\partial \log \nu_{rest} = \partial S_i/\partial \log(1+z) \simeq 0.25 - 0.3 \tag{2}$$

and is consistent with Giallongo, Trèvese & Vagnetti (1991), Cristiani et al. (1996) and Di Clemente et al. (1996). Therefore the increase of variability with redshift and its interpretation in terms of an average increase of the amplitude of variability with frequency are confirmed by the present results despite their poor statistical basis.

Hawkins (1996) finds that the variability timescale is independent of redshift, i.e. it is not affected by cosmological time dilation. He suggests that the effect can be explained in the framework of gravitational microlensing caused by intervening matter. Hawkins (2001) estimates that a possible decrease of variability *timescale* with frequency is not sufficient to compensate for the cosmological time dilation. The frequency dependence of variability *amplitude* can also compensate, at least in part, for time dilation. We note that from Eq. 2 we can estimate a vertical shift of ~ 0.1 between B and R power spectra, approximately consistent with the horizontal shift of ~ 0.06 found by Hawkins (2001) (see his Figure 3). However, a detailed evaluation of the amplitude shift of the variability power spectrum as a function of redshift would require the knowledge of the redshift, luminosity, and observing time distributions of the sample.

We also stress that the frequency dependence of microlensing (Alexander 1995) should be compared with the results shown in Fig. 2 and Eq. 2.

4. THE SPECTRAL SLOPE α AND THE SPECTRAL VARIABILITY PARAMETER β

The average increase of variability with frequency can be interpreted in terms of a change of the spectral slope with luminosity. However the statistical evidence discussed in the previous section, and in Giallongo, Trèvese & Vagnetti (1991), Di Clemente et al. (1996), is only indirect and must be confirmed by observations of individual objects in at least two bands. This was done by Giveon et al. (1999) in terms of correlation of color changes $\Delta(B-R)$ with brightness variations ΔB or ΔR and by Trèvese, Kron, & Bunone (2001) in terms of changes of the spectral slope α, defined by $L_\nu \sim \nu^\alpha$, where L_ν is the intrinsic power per unit frequency. The latter work is based on U,B_J,F, N observations at two epochs of the sample of QSOs of the Selected Area 57. The increase of spectral slope is computed as an average value over the ensemble of objects, and compared with a simple model consisting of a black body subject to small temperature changes. The data of Giveon et al. (1999), which contain on average 40 B and R observations of each QSO, allow the statistical analysis of spectral slope changes of each object, for which we compute the instantaneous slope:

$$\alpha(t) \equiv \log(L_{\nu_B}/L_{\nu_R})/\log(\nu_B/\nu_R) = -\frac{0.4[(B-R)-(B_o-R_o)]}{\log\frac{\lambda_R}{\lambda_B}} - 2, \quad (3)$$

where $m_o = -2.5 \log f_o$ are the zero points of B and R photometric bands respectively (Cox 2000). Taking into account that typical variability time scales are ≈ 1 yr (see e.g. Trèvese et al. (1994)) we regard as simultaneous the observations within a time interval of 9 hours. In Figure 3 we report the instantaneous value of the spectral slope α as a function of the intrinsic luminosity L_{ν_B}. Each small cloud of points represents a single QSO in different luminosity states. The relevant regression lines are reported on each cloud. They show, with a few exceptions, a positive correlation between the spectral slope and the intrinsic luminosity, which we call intra-QSO $\alpha - L$ correlation. The distribution of clouds in Figure 3 also shows that the average slope of each QSO tends to be larger for brighter objects, forming a sort of QSO main sequence in the $\alpha - L$ plane (Trèvese & Vagnetti 2001a). This inter-QSO $\alpha - L$ correlation can be quantified considering for each QSO the average values $\langle\alpha\rangle$ and $\langle L_{\nu_B}\rangle$ of the slope and luminosity. The correlation $r_{\alpha-L} = 0.58$ is highly significant: $P(> r) = 6 \cdot 10^{-5}$.

Figure 3 might suggest that both correlations are produced by the same physical mechanism, e.g. an increase of the temperature of the emitting gas (Trèvese, Kron, & Bunone (2001), see also Paltani & Courvoisier (1994)). However, in order to try any comparison with possible models, a precise quantification of the above effects is needed. In fact, a variety of mechanisms might in principle be responsible for a hardening of the spectrum in the bright phases. For instance, if AGNs are powered by supernovae explosions and variability is caused by a "Christmas tree" effect, then there will be an excess of blue emission in the bright phase (Aretxaga, Cid Fernandes & Terlevich 1997; Cid Fernandes et al. 2000). Even gravitational lensing (Hawkins 1996), usually thought of as achromatic, can produce a stronger variability in the blue than in the red band since the amplification depends on the size of the accretion disk which is larger in the red than in the blue band (Alexander 1995).

Also hot spots due to instabilities of the accretion disk (Kawaguchi et al. 1998) are likely to enhance the blue emission. Finally the spectral energy distribution of the host galaxy, which is redder than the AGN and gives a stronger contribution in the faint AGN phase, can produce a similar effect.

In order to quantify the spectral variations we define a spectral variability parameter

(SVP) representing the spectral slope changes per unit log-luminosity change:

$$\beta(\tau) \equiv \frac{\alpha(t+\tau) - \alpha(t)}{\log L_B(t+\tau) - \log L_B(t)}, \tag{4}$$

where $L_B(t)$ is the luminosity in the B band and τ is an appropriate time delay. In fact we expect that different physical phenomena are causing different SED changes on the relevant time scales, which go at least from days to more than ten years. With the available light curves we have computed, for each QSO, $\beta(\tau_{ij})$ with $\tau_{ij} \equiv t_i - t_j$,$i, j = 1, N$ representing all the possible time differences between the N points of the light curve. Figure 4 represents $\beta(\tau_{ij})$ for two of the 42 QSOs considered, PG0804+762 and PG1354+213, taken as examples of good and poor time sampling respectively. For each bin, the mean value of the SVP is also shown. The uncertainty is the r.m.s. variation of the mean. No obvious trend is seen looking at similar plots for the entire sample: the average β values stay almost constant, within the uncertainty, at least for $\tau \lesssim 1000$ d. Clearly, bins at large τ are less populated. An increase or decrease of β appears for some objects at larger τ where, however, the statistic becomes poor. Apparently, an analysis of possible systematic β changes on time scales $\tau \gtrsim 3$ yr requires a time base larger than the 7 yr of the present one. For the following analysis we define the SVP of each QSO as the mean value β_m in a single bin $0 < \tau < 1000$ d. Since $\beta(\tau_{ij})$ values are not independent, the above computation of the uncertainty represents an overestimate of the standard deviation of β_m. In Figure 6 β_m of the 42 QSOs are reported versus the relevant time average $\bar{\alpha}$. The curves are described in the following paragraphs, except the dot-dashed line representing a black body, which is reported for comparison with the results of Trèvese, Kron, & Bunone (2001). In the case of a black body (of fixed area), defining $x \equiv h\nu/kT$, with T, h, k equal to temperature, Planck and Boltzmann constants respectively, the spectral slope is $\alpha_{BB}(x) = 3 - xe^x/(e^x - 1)$ and the SVP is $(d\alpha/dT)/(d\log B_\nu/dT) = (\ln 10)[1 - x/(e^x - 1)] \equiv \beta_{BB}(x)$. We stress that the dotted line, defined by the above expression, does not represent a fit to the points (no free parameters). For a fixed frequency $\log \bar{\nu} \equiv \log(\nu_B \nu_R)^{\frac{1}{2}}$ and increasing temperature, a point moves on the curve from left to right (Rayleigh-Jeans limit $\alpha = 2, \beta = 0$). The "average QSO", $\langle\bar{\alpha}\rangle = -0.2 \pm 1.0, \langle\beta_m\rangle = 2.2 \pm 0.9$, can be represented by temperature changes of a black body of $T \approx 10^4$ K, in approximate agreement with the result of Trèvese, Kron, & Bunone (2001), which was obtained with different QSO sample and mean rest-frame frequency.

5. THE EFFECT OF THE HOST GALAXY

An independent analysis of the same light curves, performed by Cid Fernandes et al. (2000) in the framework of Poissonian model of variability, implies the existence of an underlying spectral component, redder than the variable one, which could be identified either with the non-flaring part of the QSO spectrum or with the host galaxy considered by Romano & Peterson (1998). We evaluate the effect of the host galaxy through numerical simulations based on templates of the QSO and host galaxy SEDs (Trèvese & Vagnetti 2001b). Both SEDs are derived from the atlas of normal QSO continuum spectra of Elvis et al. (1994). We compute a synthetic QSO+host spectrum, adding to the fixed host galaxy template SED the average QSO spectrum with a relative weight characterized by the parameter $\eta \equiv \log(L_H^Q/L_H^g)$, where L_H^Q and L_H^g are the total H band luminosities of the QSO and the host galaxy respectively. In the Elvis et al. (1994) sample, η ranges from -1 to 2. Figure 5 shows an example of composite spectrum. We want to test (disprove) the hypothesis that the QSO SED maintains its shape during brightness changes, while the variation of the spectral shape is entirely due to the contribution of the (constant) galaxy SED. We know that the effect of the host galaxy should be small in the case of Giveon et al. (1999) data since: i) magnitudes were computed using point spread function fitting of the images, ii) the images were limited by an aperture with the diameter depending on the seeing conditions, but smaller than 3 arcsec. However we don't know the appropriate value of η. For this reason we perform simulations for a range of η values. Variability is represented by small changes $\Delta\eta$, around each η value, with an amplitude corresponding to a r.m.s. variability $\sigma_B = 0.16$ mag in the blue band. For each synthetic spectrum, representing the QSO plus host SED at a given time, we compute $\alpha(\bar{\nu}, t) \equiv (\partial \log L_\nu / \partial \log \nu)_{\nu=\bar{\nu}}$, $\bar{\nu} = \sqrt{\nu_B \nu_R}$, then we derive the SVP β. The result, for $-3 < \eta < 3$, is shown in Figure 6. To check the dependence of the result on QSO redshift, the same computation is repeated for the maximum redshift of the Giveon et al. (1999) sample, $z = 0.4$, and shown in the same figure. Although an appropriate choice of η can reproduce the observed β or α separately, the curves are clearly shifted respect to the distribution of the observational points. This means that the effect of the host galaxy is not sufficient to account for the observed changes of the spectral shape. Thus the spectral variability is intrinsic of the active nucleus. This also implies that the constant red continuum, resulting from the analysis of Cid Fernandes et al. (2000), cannot be identified with the host galaxy. It must be, at least in part, due to the nucleus, and can be identified with the spectrum of the non-flaring part of the accretion disk.

6. CHANGES OF $\dot{M}$ AND "HOT SPOTS"

Once the spectral variability is ascribed to the nuclear component, we can ask whether a change of any of the parameters defining an emission model can account for the observed variations of the spectral shape . We considered the accretion disk model of Siemiginowska et al. (1995), Fiore et al. (1995), corresponding to a Kerr metric and modified black body SED, which depend on the black hole mass M, the accretion rate $\dot{M}$ and the inclination θ

($\theta = 0 \rightarrow$ face-on). A grid of models has been considered for $\log M/M_{\odot} = 7.0, 8.0, 9.0, 10.0$, $\dot{m} \equiv \dot{M}c^2/L_E = 0.1, 0.3, 0.8$ (where L_E is the Eddington luminosity $L_E = \frac{4\pi Gcm_p}{\sigma_e M}$ with the usual meaning of symbols) and $\mu \equiv \cos\theta = 1, 0.75, 0.5, 0.25, 0.1$. A change of $\dot{M}$ produces a variation of both luminosity and the SED shape. On purely theoretical grounds, we know that the time required for the accretion disk to reach a new equilibrium condition with a different $\dot{M}$ value is at least of the order of the sound crossing time $t_{sound} \approx 10^3 - 10^5$ d (Courvoisier 1991), i.e. much longer than typical variability time scales. Still, it is interesting to see how the spectral changes between two $\dot{M}$ states compare with the observed ones, as done by Tripp, Bechtold & Green (1994), and by Siemiginowska et al. (1995). In Figure 6 the two curves on the bottom right represent β versus α for varying M (from right to left) as computed for two different values of $\dot{m}$ and for $\mu = 1$, from the Kerr metric, modified black body model of Siemiginowska et al. (1995) (their table 4). The spectral variations are clearly smaller, on average, than the observed ones. This means that a transition e.g. from a lower to a higher $\dot{M}$ regime implies a larger luminosity change for a given slope variation. Notice that a black body of varying T and fixed area provides larger β values consistent with the observations. Thus, β values computed for an increase of $\dot{m}$ would better compare with the case of a transition to a hotter disk with larger area. Observed slope variations of two objects, NGC 5548 and NGC 3783, have been compared with the predictions of an accretion disk model by Tripp, Bechtold & Green (1994), in the UV range. They conclude that the observed points lie roughly on curves of constant black hole mass, giving confidence in the accretion disk models. However we notice that also in this case the distribution of observed points is steeper than the iso-mass lines, specially in the case of NGC 3783. Our result on the statistical sample of 42 objects indicates that this is indeed a systematic effect.

This result suggests that transient phenomena, like hot spots produced on the accretion disk by instability phenomena (Kawaguchi et al. 1998), instead of a transition to a new equilibrium state, may better explain the relatively large changes of the local spectral slope, The available models of instability phenomena do not provide a spectrum of the hot spot. Thus we try a simple “model” based on the addition of a black body flare to the disk SED, represented by the average QSO SED of Elvis et al. (1994) (shown in Figure 5). The free parameters are temperature T_{BB}, and emitting area A, while the constraints are the amplitude of the luminosity change (e.g. in the B band) and the relevant β value (or the relevant $\Delta\alpha$). The solution is not univocal, given the spread of the observed β values. However, $\Delta B = 0.16$ mag (corresponding to the r.m.s. variability of the sample) can be obtained by a hot spot of $T_{BB} \approx 2 \cdot 10^5$ K and $A = 5 \cdot 10^{30}$ cm^2, producing $\beta = 3.2$, or $T_{BB} \approx 2 \cdot 10^4$ K, $A = 1,3 \cdot 10^{32}$ cm^2, giving $\beta = 2.2$. This is shown by the large filled squares in Figure 6. A sudden heating of a fraction of the disk surface is thus capable of producing the observed change of the SED in the B and R bands and the relevant intra-QSO α-L correlation.

7. SUMMARY AND CONCLUSIONS

We have performed a new analysis of the B and R light curves of a sample of 42 PG QSOs made available by the Wise Observatory group (Giveon et al. 1999). We have shown the existence of a positive v-z correlation when the analysis is restricted to a small luminosity bin.

This correlation disappears in the sample as a whole due to the interplay of v-L, L-z and v-z correlations and the small redhift range. The slope of the v-z relation is consistent with the previous findings of Di Clemente et al. (1996) and Trèvese, Kron, & Bunone (2001), thus confirming that the v-z correlation can be entirely explained by the increase of variability with frequency, coupled with the increase of (rest-frame) observing frequency for higher redshift objects. The dependence of variability on redshift has been questioned in the past (see table 1 of Giveon et al. (1999) for a summary of previous variability studies). We stress that: i) it is a relatively weak effect ($\partial v/\partial z \approx 0.1$) so that it cannot be detected unless other competing effects (including v-L and z-L correlations) are properly taken into account; ii) to get rid of spurious effects connected with cosmological time dilation and finite sampling time, variability must be quantified by an intrinsic index defined on the basis of the rest frame structure function. Once these prescriptions are adopted, the v-z correlations as measured in different optical-UV bands and different QSO samples appear consistent. This was already found by Di Clemente et al. (1996) and Trèvese, Kron, & Bunone (2001). The present evidence, though marginal, is again quantitatively consistent and confirms previous results.

The two-color light curves of the Giveon et al. (1999) sample allow for the first time the statistical analysis of SED variability of individual QSOs and the study of the spectral slope changes among QSOs of different luminosity, leading to the evidence of an intra-QSO and an inter-QSO correlation.

We have analyzed the spectral variability by the distribution of the parameter $\beta(\tau) \equiv \frac{\alpha(t+\tau)-\alpha(t)}{\log L_B(t+\tau)-\log L_B(t)}$ as a function of the spectral slope α. We have compared with the observed distribution the spectral slope changes produced by the contribution of the host galaxy to the QSO SED, under the assumption that the nuclear spectrum maintains its shape while changing its brightness. We conclude that the host galaxy alone cannot be responsible for the observed spectral changes. Thus the spectral variation must be intrinsic of the nuclear component. The β-α distribution has been also compared with the SED changes of a disk model for $\dot{M}$ variations. The latter appear insufficient to explain the observed spectral changes. Bright spots on the disk, likely produced by local instabilities, are able to represent the observed spectral variability.

Since it is likely that different physical phenomena are causing variability in different bands and time scales, multi-frequency analyses will be ultimately needed to obtain a complete description. However even a two optical bands analysis, once performed on a statistical sample, provides valuable constraints on the origin of variability. This strongly suggests to extend the work of the Wise Observatory group both in frequency and sampling time to allow a more detailed comparison with possible models.

We are grateful to the Wise Observatory Group for promptly making available their data to the community, and for providing us with details about the observations. We are indebted to Fabrizio Fiore for his help in the use of disk models and for clarifying discussions. This research has made use of the NASA/IPAC Extragalactic Database (NED) which is operated by the Jet Propulsion Laboratory, California Institute of Technology, under contract with the National Aeronautics and Space Administration.

REFERENCES

Alexander, T., 1995, MNRAS, 274, 909

Angione, R. J., & Smith, H. J., 1972, in IAU Symp 44, External Galaxies and Quasi-Stellar Objects, ed. D. S. Evans, (New York: Springer-Verlag), p.171

Aretxaga, I., Cid Fernades, & Terlevich, R., 1997, MNRAS, 286, 271

Bershady, M. A., Trèvese, D., & Kron, R. G. 1998, ApJ, 496, 103

Bonoli, F., Braccesi, A., Federici, L., & Zitelli, V., 1979, A&AS, 35, 391

Cid Fernandes, R., Sodrè, L., Jr. Vieira da Silva, L., Jr., 2000 ApJ, 544, 123

Courvoisier, T. J.-L., 1991, Clavel, J., A&A, 248, 389

Courvoisier, T. J.-L., 1998, A&A Rev., 9, 1

Cox, A. N., 2000 “Allen’s Astrophysical Quantities” (Berlin: Springer-Verlag)

Cristiani, S., Vio, R., & Andreani, P. 1990, AJ, 100, 56

Cristiani, S., Trentini, S., La Franca F., Aretxaga, I., Andreani, P, Vio, R., & Gemmo A. 1996, A&A, 306, 395

Cutri, R. M., Wisniewski, W. Z., Rieke, G. H., & Lebofski, H. J. 1985, ApJ, 296, 423

Di Clemente A., Natali G., Giallongo E., Trévese D., Vagnetti F. 1996, ApJ, 463, 466

Edelson, R.A., Krolik, J. H.,& Pike, G. F. 1990, ApJ, 359, 86

Elvis, M., Wilkes, B. J., McDowell, J. C., Green, R. F., Bechtold, J., Willner, S. P., Oey, M. S., Polomski, E., Cutri, R., 1994, ApJS, 95, 1

Fiore, F., Elvis, M., Siemiginowska, A., Wilkes, B.J., McDowell, J.C., & Mathur, S.: 1995, ApJ, 449, 74

Giallongo E., Trèvese D., Vagnetti F.: 1991, ApJ, 377, 345

Giveon, U., Maoz, D., Kaspi, S., Netzer, H., & Smith P. S. 1999, MNRAS, 306, 637

Kawaguchi, T., Mineshige, S., Umemura, M., & Turner, E. L. 1998, ApJ, 504, 671

Kinney, A. L., Bohlin, R.C., Blades, J. C., & York, D. G. 1991, ApJS, 75, 645

Hawkins, M. R. S., 1983, MNRAS, 202, 571

Hawkins, M. R. S., 1996, MNRAS, 278, 787

Hawkins, M. R. S., 2001, ApJ, 553, L97

Hook, I. M.,McMahon R. G., Boyle, B. J., & Irwin, M. J. 1994, MNRAS, 268, 305

Koo, D.C., Kron, R.G., Cudworth K.M.: 1986, PASP, 98, 285

Kaspi, S., Smith, P. S., Netzer, H., Maoz, D., Jannuzi, B. T., & Giveon, U., 2000, ApJ, 533, 631

Paltani, S., & Courvoisier, T. J.-L. 1994, A&A, 291, 74

Romano, P., & Peterson, B. M., 1998, ASP Conf. Ser. 175, 55

Siemiginowska, A. Kuhn, O., Elvis, M., Fiore, F., McDowell, J., & Wilkes, B., 1995, ApJ, 454, 77

Torricelli-Ciamponi, G., Foellmi, C., Courvoisier, T. J.-L., & Paltani, S., 2000, A&A, 358, 57

Trèvese, D., Kron, R. G., & Bunone A., 2001, ApJ, 551, 103

Trèvese, D., Kron, R. G., Majewski, S. R., Bershady, M. A., Koo, D. C. 1994, ApJ, 433, 494

Trèvese D., Pittella G., Kron R. G., Koo D. C., & Bershady M. A. 1989, AJ, 98, 108

Trèvese, D., & Vagnetti, F., 2001a in 'Guillermo Haro Advanced Lectures on the Starburst-AGN Connection', R. Mujica et al. Eds., INAOE Electronic Edition (http://www.inaoep.ms/∼agn00/posters.html), pp. 101-103

Trèvese, D., & Vagnetti, F., 2001b, in 'QSO Hosts and their Environments', I. Marquez et al. Eds., in press (astro-ph/0102252)

Tripp, T. M., Bechtold, J., & Green, R. F., 1994, ApJ, 433, 533

Ulrich, M. H., Maraschi L., & Urry C. M. 1997, ARA&A, 35, 445

Fig. 1.— Variability S_B (0.3±0.09 yr) versus redshift for the subsample with $-23.5 < M_B < -22.5$. The correlation coefficient r and the relevant probability (of the null hypothesis) are also reported.

Fig. 2.— Variability S versus rest-frame frequency for various QSO samples (adapted from Di Clemente et al. (1996)). The variability indicator is the ensemble average of variability indexes over the relevant QSO samples. The frequencies of each point are defined as the relevant ensemble averages of the rest-frame QSO frequencies, according to the individual redshift and observing band. Filled symbols correspond to $\tau = 0.3 \pm 0.09$ yr and open symbols correspond to $\tau = 2.0 \pm 0.3$ yr. The stars represent the four variability indexes of the present analysis.

Fig. 3.— Instantaneous spectral slope α versus monochromatic luminosity L_{ν_B}. Regression lines $\alpha - L_{\nu_B}$ are reported for each QSO. Dotted curves represent black bodies of different areas with temperature T increasing from bottom left to top right (Rayleigh-Jeans limit $\alpha = +2$).

Fig. 4.— The spectral variability parameter $\beta(\tau_{ij})$ as a function of the time lag between the observations for PG0804+762 and PG1354+213. Filled circles represent the mean value of $\beta(\tau_{ij})$ in intervals of 500 d. Error bars represent the r.m.s. uncertainty of the mean.

Fig. 5.— Synthetic spectra (thin continuous lines) resulting from the composition of the average QSO spectrum (dotted lines) and the host galaxy template spectrum (thick line), both taken from Elvis et al. (1994), $\eta \equiv \log(L_H^Q/L_H^g) = -1, 0, 1$

Fig. 6.— The spectral variability parameter β_m (see Eq. 4) versus the average spectral slope for each QSO of the sample. Error bars represent the r.m.s. statistical uncertainties, which are mainly due to intrinsic variability. Dot-dashed line: sequence of black bodies of different temperatures (increasing from left to right); continuous line: spectral variability due to the presence of the host galaxy, in the QSO rest-frame, for η ranging from -3 (left) to 3 (right); dotted line: the same as continuous line, for a QSO at the maximum redshift of the sample, $z = 0.4$; thick continuous line: spectral variability caused by an increase of $\dot{m} \equiv \frac{\dot{M}}{\dot{M}_{Edd}}$ from 0.1 to 0.3 in the model of table 4 of Siemiginowska et al. (1995) (Kerr + modified black body), M increasing from 10^7 to 10^{10} $M_\odot$ (from right to left); thick dashed line: the same as above for $\dot{m}$ increasing from 0.3 to 0.8. Large filled squares represent the hot spot model for $T = 2 \cdot 10^5$ K (upper) and $T = 2 \cdot 10^4$ K (lower) (see text).

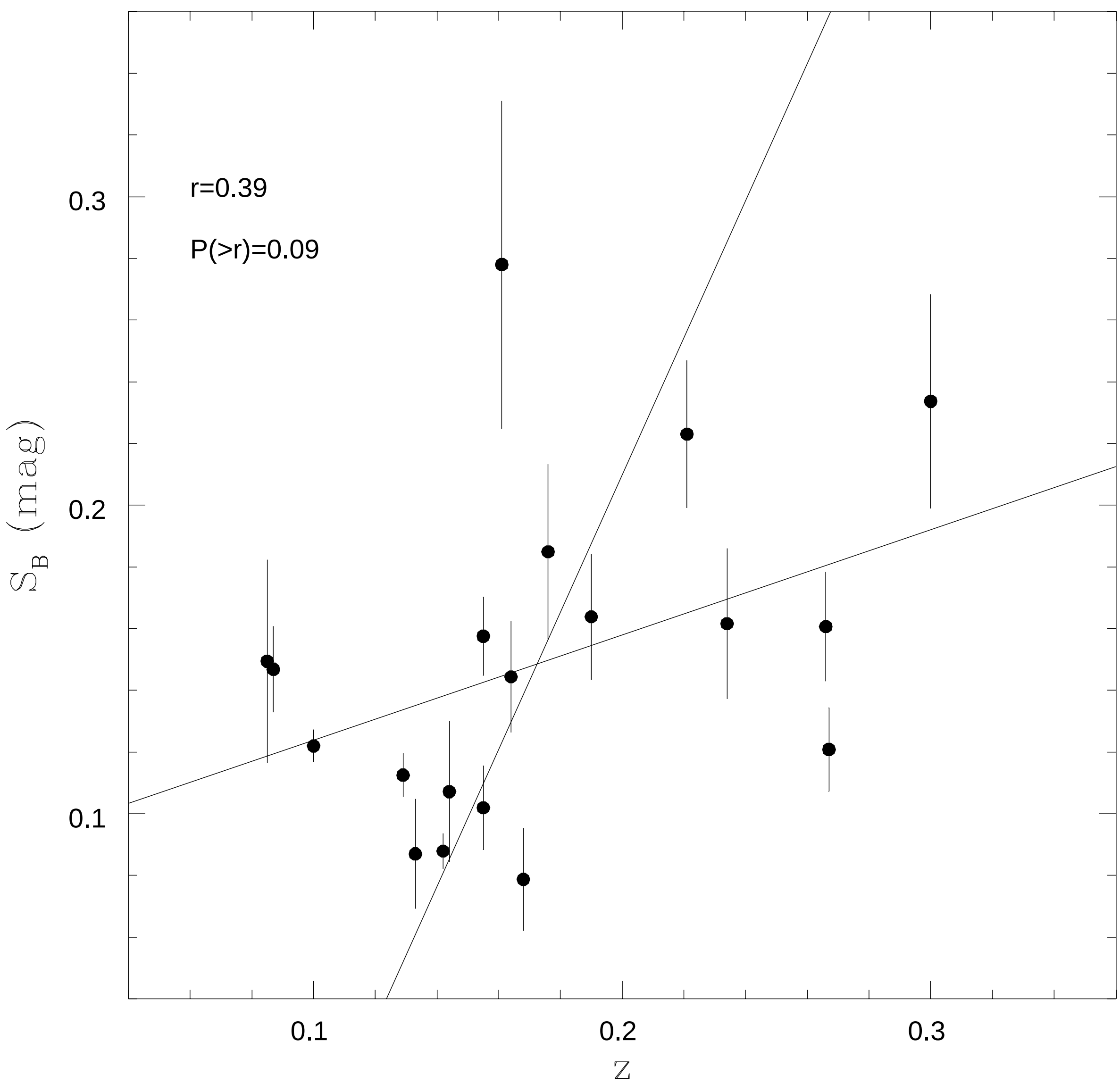

r=0.39
P(>r)=0.09
0.3
0.2
0.1
S_B (mag)
0.1
0.2
0.3
z

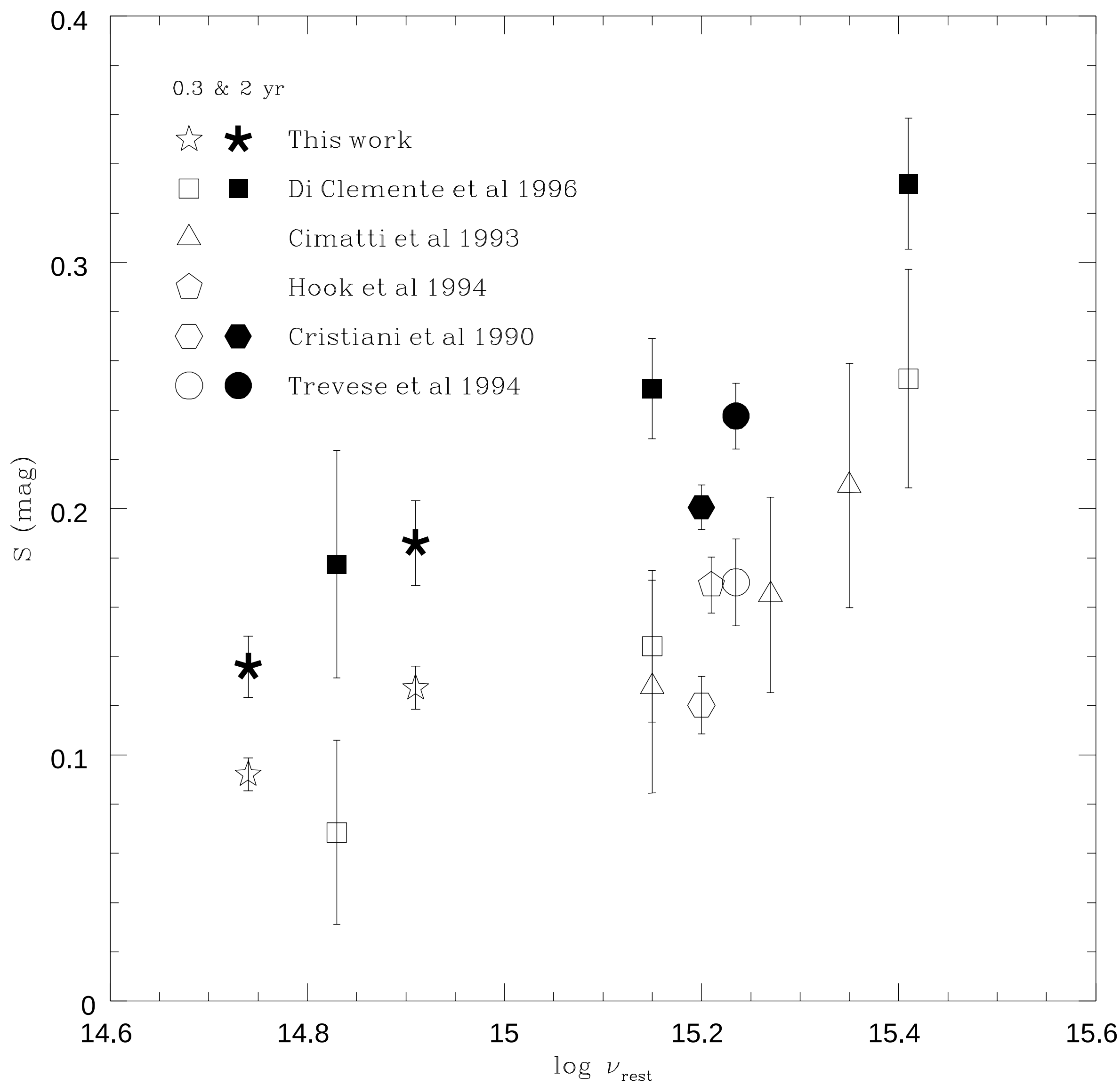

0.3 & 2 yr
This work
Di Clemente et al 1996
Cimatti et al 1993
Hook et al 1994
Cristiani et al 1990
Trevese et al 1994
S (mag)
log ν rest
0
0.1
0.2
0.3
0.4
14.6
14.8
15
15.2
15.4
15.6

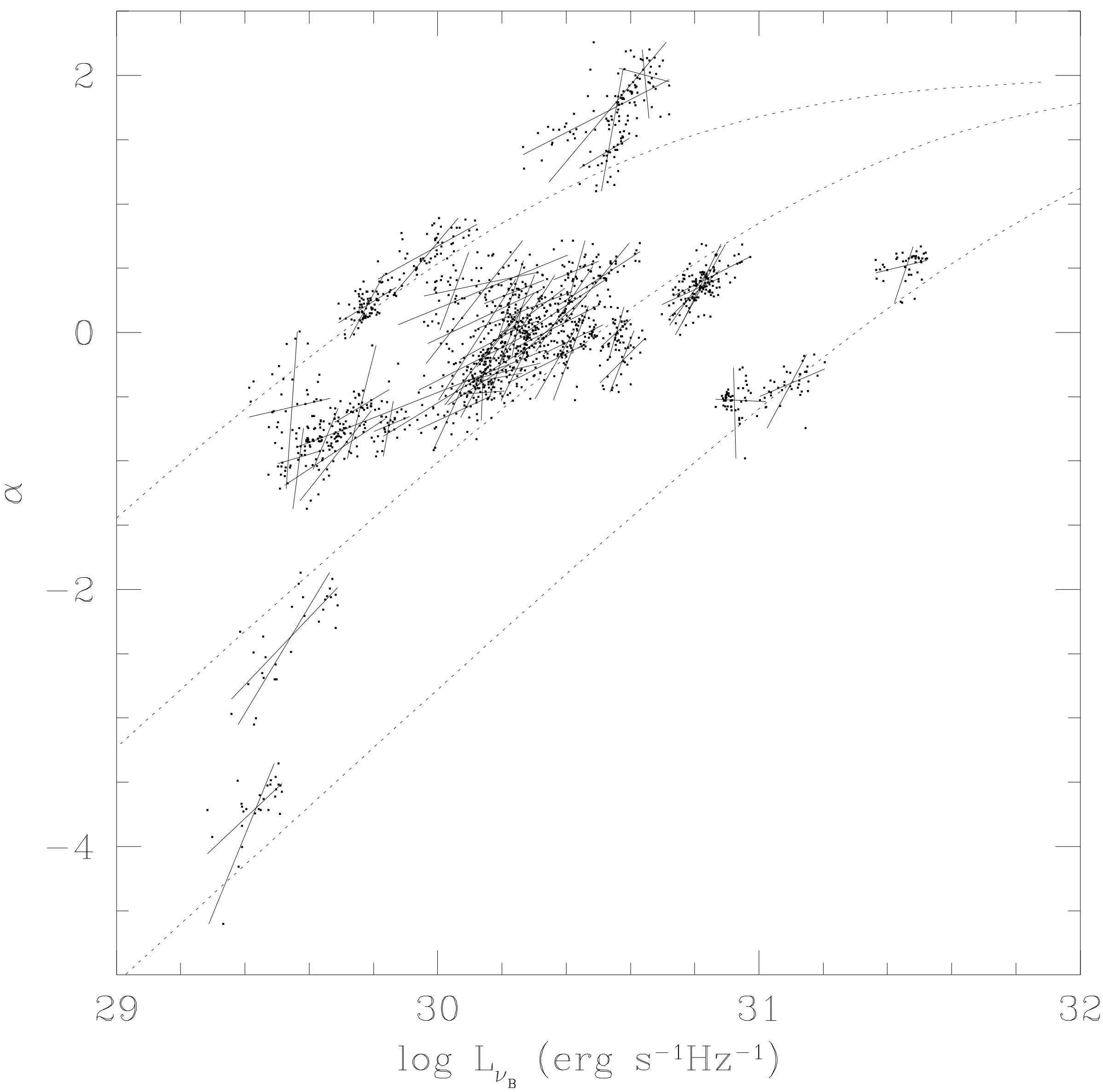
2
0
−2
−4
α
29
30
31
32
log L_{ν_B} (erg $s^{-1}Hz^{-1}$)

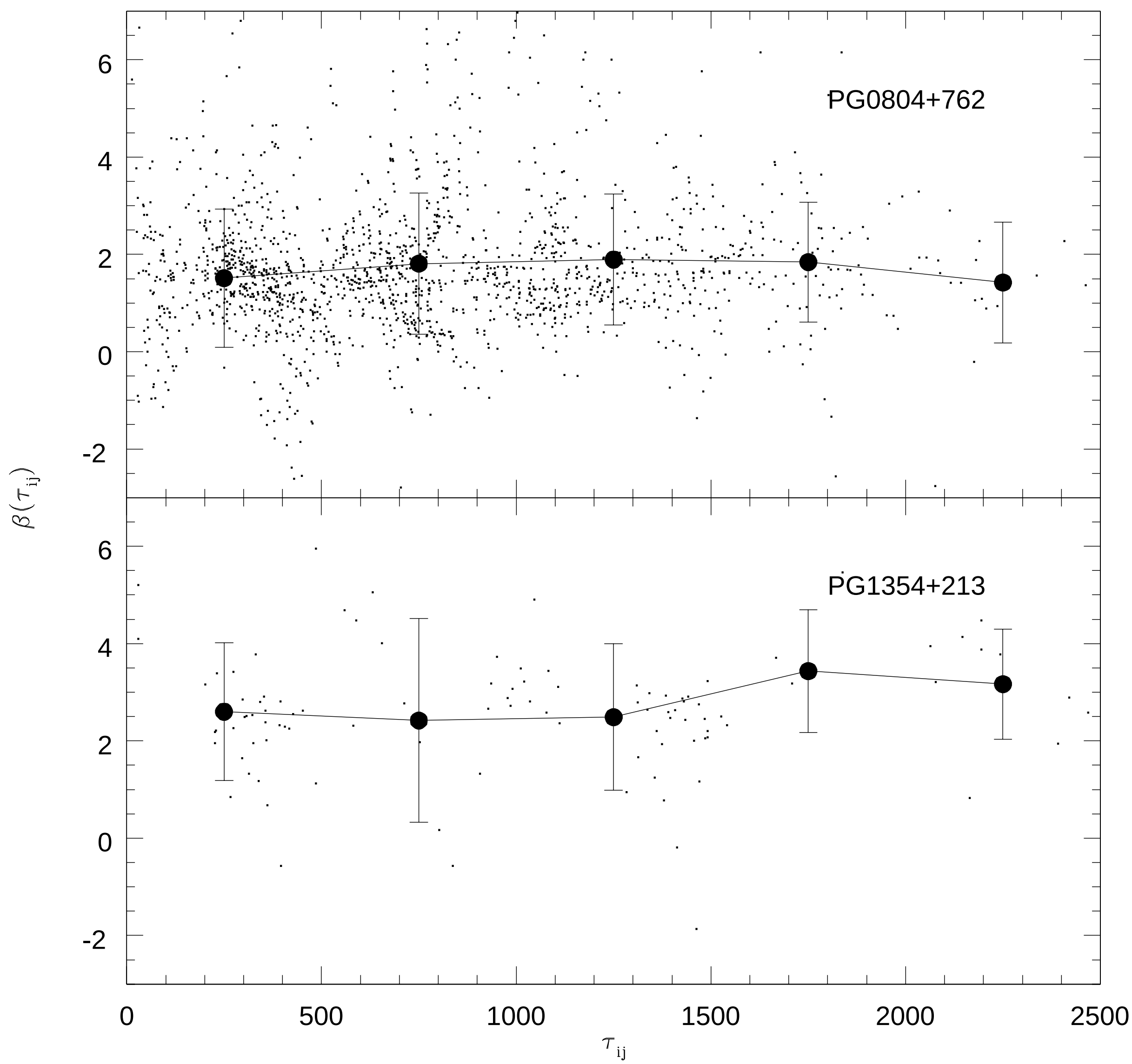
PG0804+762
PG1354+213
$\beta(\tau_{ij})$
τ_{ij}
6
4
2
0
-2
0
500
1000
1500
2000
2500

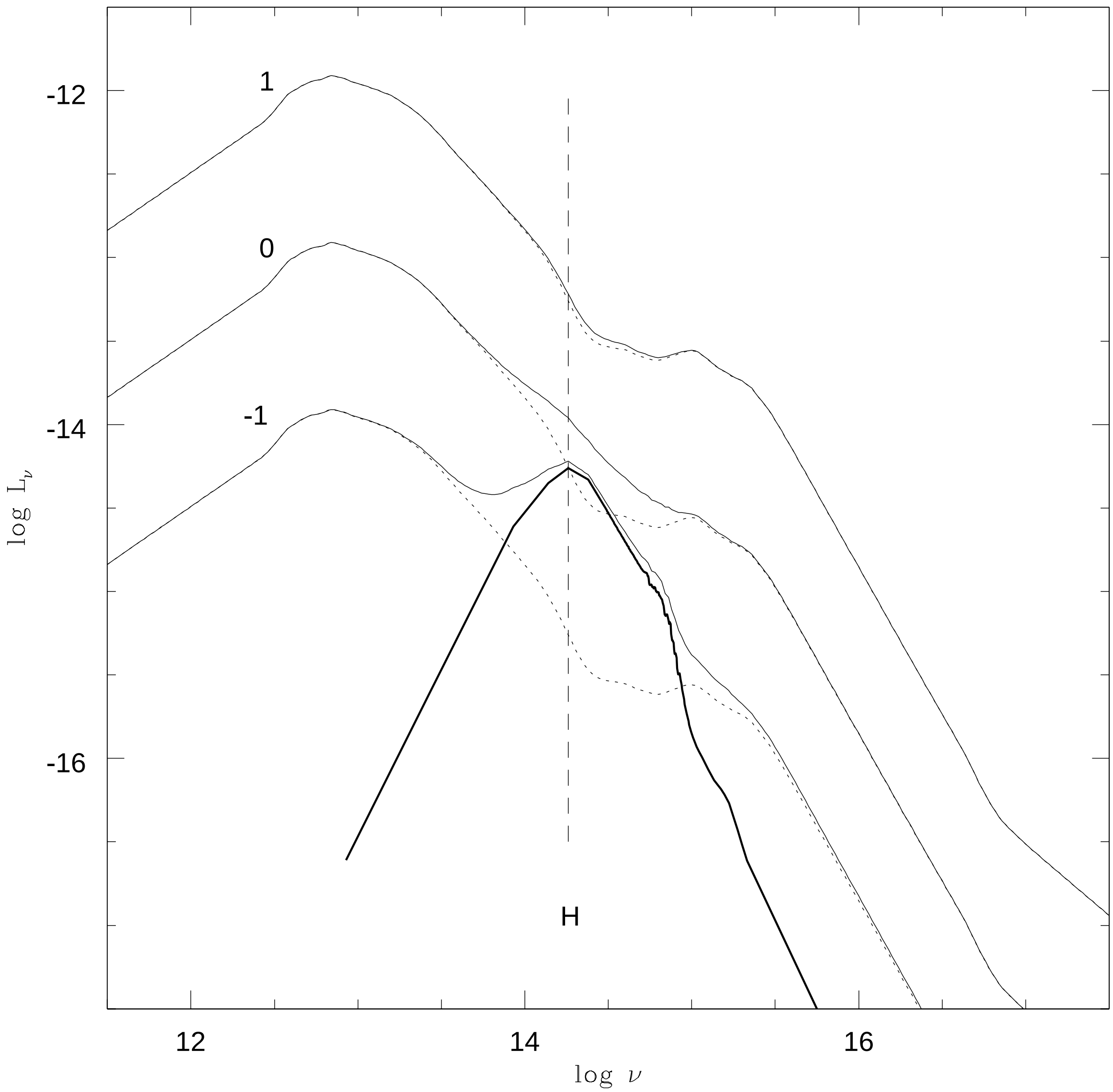
1
0
-1
H
-12
-14
-16
log L_ν
12
14
16
log ν

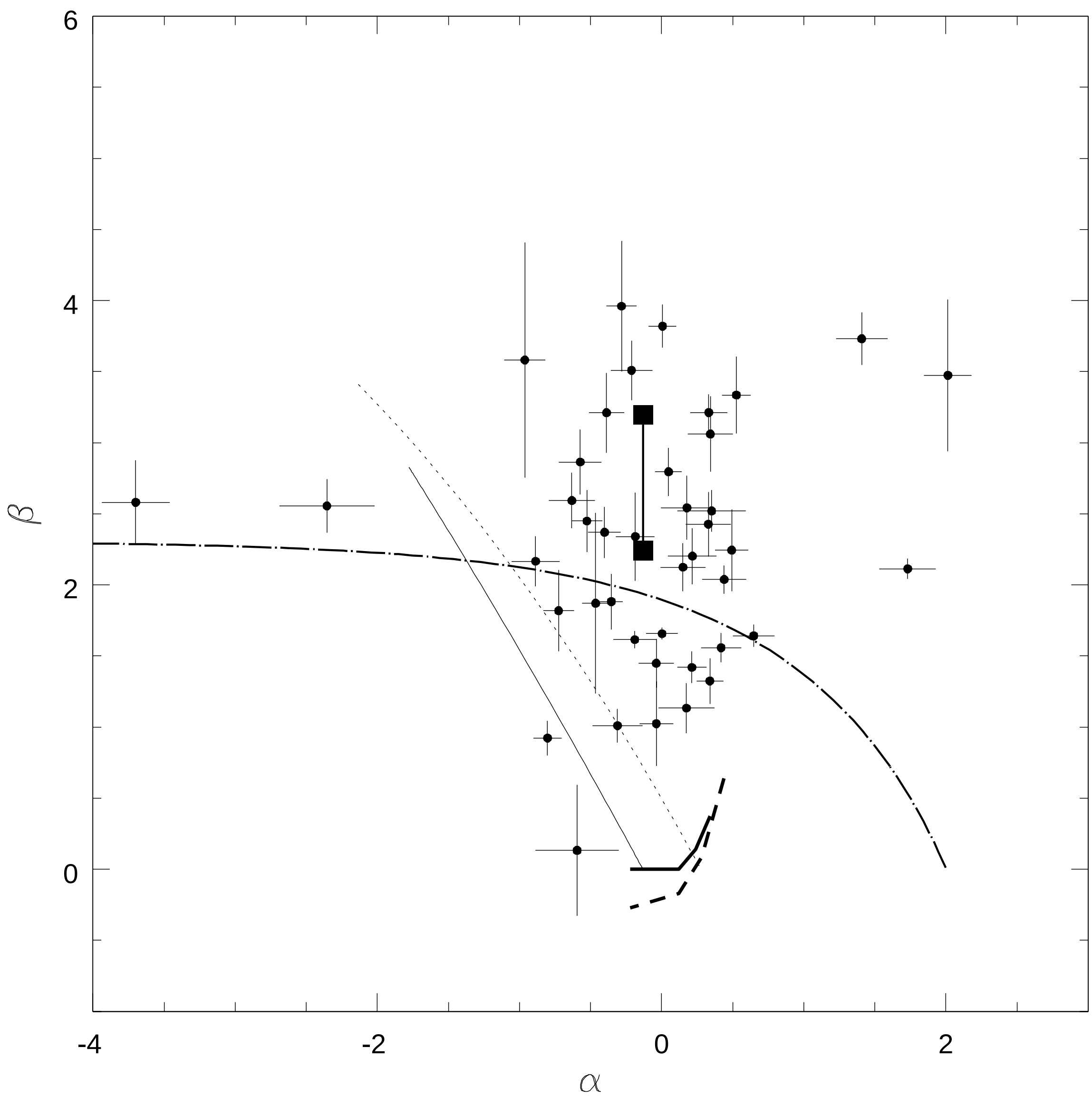

6
4
2
0
-4
-2
0
2
β
α